Hindawi
Scientific Programming
Volume 2023, Article ID 1149108, 14 pages
https://doi.org/10.1155/2023/1149108

Research Article

Changing Properties of Daily Precipitation Concentration in the Hai River Basin, China

Ren Zheng[1,2] **Zhao Yong**[3] **Chen Ling**[4] **Gong Jiaguo**[3] **and Wang Li**[1,2]

[1]*School of Water Conservancy and Hydroelectric Power, Hebei University of Engineering, Handan, China*
[2]*Hebei Key Laboratory of Intelligent Water Conservancy, Hebei University of Engineering, Handan, China*
[3]*State Key Laboratory of Simulation and Regulation of Water Cycle in River Basin, China Institute of Water Resources and Hydropower Research, Beijing, China*
[4]*School of Management Engineering and Business, Hebei University of Engineering, Handan, China*

Correspondence should be addressed to Zhao Yong; zhaoyong@iwhr.com

Received 5 July 2022; Revised 30 November 2022; Accepted 13 December 2022; Published 6 February 2023

Academic Editor: Pengwei Wang

Understanding the spatiotemporal pattern of precipitation concentration is important for the assessment of flood and drought risk and utilization of water resources. In this study, the daily precipitation concentration index in the Hai River basin in China was calculated based on the Gini coefficient obtained from the observed data of 51 meteorological stations from 1951 to 2018 and spatiotemporal pattern variations were investigated. The trends and abrupt changes of DPCI were tested by the Mann–Kendall and the Pettitt methods, respectively. The relationships among DPCI, percentage of precipitation contributed by the rainiest days, and disaster losses were discussed by the linear correlation analysis. The results showed that the DPCI value ranges between 0.6471 and 0.7938, decreases westward and northward, which is negatively related to latitude and elevation, and is positively related to longitude. Negative trends of the DPCI were found at most stations, and the PCI trends of more than 80% stations were statistically significant. Abrupt changes of the DPCI have a postponement trend from west to east with time. Daily heterogeneity of the rainfall in a year is highly correlated with the heavy rainfall amount of the 25% rainiest days. For a year, higher DPCI coupled with more precipitation is easy to cause a flood disaster; conversely, higher DPCI along with less precipitation is easy to cause a drought disaster. In the future, the risk of flood disasters would be reduced, but the drought disasters would be increased in the Hai River basin.

1. Introduction

The study regarding climatic variables has received considerable attention from researchers throughout the world. In general, there are two main climatic variables, which are temperature with cold and warm changes and precipitation with dry and wet changes [1–3]. Precipitation, as an important factor in the water cycle, determines the availability of water resources, the type and extent of agriculture, and natural physical phenomena [4]. With climate warming, precipitation intensity, amounts, and patterns are expected to change, and natural disasters are likely to occur more frequently [5–7]. Precipitation extremes, such as heavy precipitation events occurring over very few days that account for high percentages of the annual total, are directly responsible for flood occurrences and will bring more frequent disasters for human society [8]. One typical example of the daily precipitation concentration degree involved in the precipitation in Henan province of China on 20 July, 2021, when the equivalent fell of what exceeds 40% of the annual total precipitation. The flood involved 14.786 million people of 150 regions in Henan province, and the direct economic loss reached 120.06 billion yuan. Thus, the analysis of daily precipitation concentration is an important issue in climate research and can be useful to evaluate risks linked to extreme precipitation events [9].

The daily precipitation concentration index (DPCI) is an index for describing the varying involvement of daily

precipitation, considering the contribution of days with the greatest amount of precipitation to the total amount of precipitation [10]. Higher values of precipitation concentration in a certain region mean that precipitation amount would mostly concentrate within a shorter period of time. Since the DPCI has been developed by Cortesi et al., it has been widely used in the analysis of precipitation concentration in Europe [11], Peninsular Malaysia [12], Iran [8, 13], Southern Russia [14], Central-Southern Chile [4], Puerto Rico [15], and Central Asia [16]. In China, spatial and temporal variabilities of DPCI have been investigated in different regions. However, systematic differences exist. On the basis of 40 sites in the Pearl River basin measured during 1960–2005, Zhang et al. identified lower and decreasing DPCI in the southwest and northeast parts, but higher and increasing DPCI in the northwest and south parts [17]. The study by Li et al. showed that higher DPCIs were mainly observed in Southern Xinjiang, whereas lower DPCIs were mostly detected in Northern Xinjiang. The most parts of Xinjiang are characterized by no significant trends of DPCI at the 0.05 significance level [18]. Shi et al. found that the lowest DPCIs occurred mainly in the upper reaches of the Lancang River basin, where a significant and negative trend in DPCI that exceeding the 95th percentile was also detected [10]. However, positive trends in the DPCI were found at most stations in the upper reaches of the Huai River basin, although none of the DPCI trends were statistically significant [19]. Yuan et al. also discussed the trends of DPCI in Shanxi province and showed that there were negative trends of DPCI with larger trends in the plain area than in the alpine area [20]. Wang et al. discovered spatiotemporal changes of the DPCI in Northeast China, where the DPCIs decreased slightly in most areas and the regions of the highest value were in Liaoning province [21]. More recently, Mei et al. examined changes to the distribution of the DPCI from 36 meteorological stations in the Yangtze River Delta from 1960 to 2017, and they found that DPCIs of 22 stations (accounting for 61%) showed increasing trends, while three stations increased significantly at the 95% significant level [22].

The Hai River basin (HRB) is of particular interest because it is an important water source for Beijing, the capital of China, and Xiong'an New Area, a national new area. Understanding the effects of spatial-temporal variations in the precipitation concentration index in the HRB is a key to urban water resources management, especially in the context of climate change and human activities. A few studies have addressed these changes in precipitation within the HRB. These studies identified precipitation trends during the annual and seasonal spells [23], as well as extreme precipitation events [24, 25]. However, few studies have analyzed the contribution of daily rainstorm to total precipitation amount of a certain spells. Investigating the DPCI in the HRB could provide a solid basis for analyzing the relationship between water resources and climate change within the basin. At the same time, this investigation would provide support for making decisions about water resource allocation in the middle route of the South-to-North Water Transfer project and for urban construction to reduce risks of urban flood-induced impacts. The main purpose of this paper is to explore (i) the spatial pattern variations of daily precipitation concentration; (ii) temporal trends and abrupt changes of daily precipitation concentration; and (iii) the relationship between daily precipitation distribution in a year and percentage of precipitation contributed by the rainiest days. This paper is organized as follows. Section 2 describes the study area and data employed in this study. Section 3 introduces the DPCI and other methods involved in this paper. The results and discussion are presented in Sections 4 and 5, respectively. Finally, conclusions are drawn in Section 6.

2. Study Area and Data

2.1. Study Area. The HRB (Figure 1), the most important grain-production regions in northern China, lies between approximately 112° E and 120° E and 35° N and 43° N [26]. The basin includes most or part of eight provincial administrative regions (Beijing, Tianjin, Hebei, Shanxi, Henan, Shandong, Inner Mongolia, and Liaoning) and has an area of about 318,000 km^2, which accounts for 3.3% of the entire land area of China [27]. The basin has been the political, economic, and cultural center of China since ancient times and has a current population of 154 million, accounting for 11% of China's total population. There are eight main tributaries (Luan River, Jiyun River, Chaobai River, Yongding River, Daqing River, Ziya River, Nanyun River, and Majia River) that flow eastward to the Sea of Bohai with elevations ranging from 0 to 3024 m above the mean sea level based on a digital elevation model (30 m × 30 m grids) of the basin.

The climate of the HRB, determined by the monsoon, is typically semi-humid and semiarid [26]. In the wet season (May–October), the influence of southwest monsoon from the Bay of Bengal and southeast monsoon from the West Pacific favors large amounts of precipitation. In contrast, the dry season (November–April) is prone to serious drought. Therefore, there is an uneven distribution of precipitation throughout the year. The average annual precipitation in the basin is about 548 mm, which is mainly concentrated in the wet season. Moreover, about 80% of the annual precipitation occurs in the flood season from June to September [27].

2.2. Data. The daily precipitation data for the HRB and its surroundings are provided by the National Climatic Center (NCC) of the China Meteorological Administration (CMA) and can be downloaded from https://data.cma.cn/data/cdcindex/cid/6d1b5efbdcbf9a58.html. Within the HRB, daily precipitation data at 51 meteorological stations, the locations of which are shown in Figure 1, are used to analyze the temporal and spatial variability of daily precipitation concentration (Table 1). The longest time series of daily precipitation data among 51 meteorological stations are 68 years from 1951 to 2018. In contrast, the shortest time series are 46 years from 1973 to 2018. To ensure data continuity and integrity, the daily precipitation data gaps at a specific station were interpolated by an inverse distance

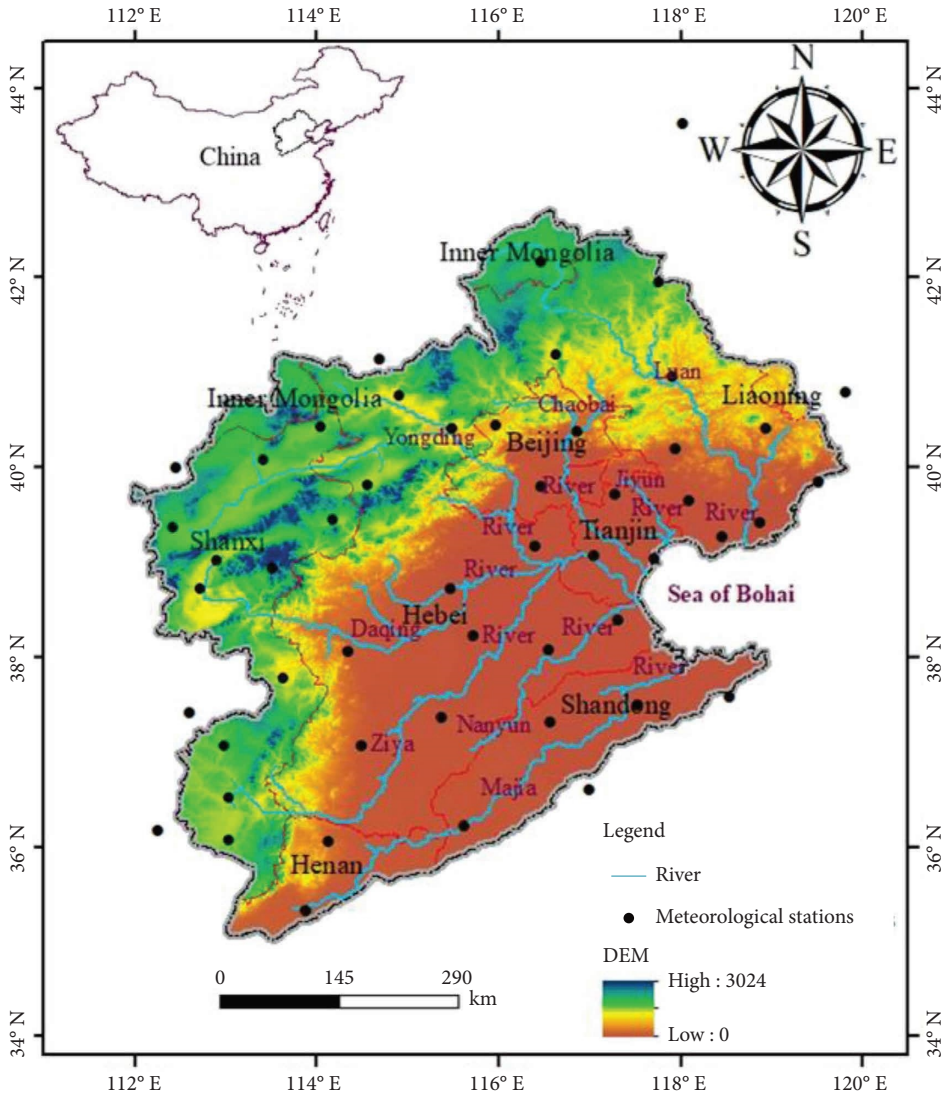

Figure 1: Location of meteorological stations in the Hai River basin.

weighting (IDW) [28] based on data from adjacent meteorological stations and thus daily precipitation data of 51 stations were all extended to the period of 1951–2018.

The loss data of flood and drought disasters in the HRB comes from the "flood and drought disasters in the Haihe River Basin" composed by the Haihe River Water Conservancy Commission, Ministry of Water Resources of the People's Republic of China (MWR) [29].

3. Methodology

3.1. DPCI Calculation. The DPCI is an important indicator that is used to evaluate the relative importance of the daily precipitation classes, especially the contribution of the largest daily event to the total amount and the cumulative percentage of precipitation contributed by the cumulative percentage of days when precipitation occurred [4]. Among many daily precipitation concentration indices, the Gini coefficient (GC) was recommended to characterize daily precipitation concentration [30]. Generally, the GC with a range from 0 to 1 is a common indicator used to measure the income/wealth gap of residents in a country or region [31]. The greater GC means the greater national income gap. In this paper, the GC was used to measure daily precipitation concentration, and the DPCI can be calculated as follows [16, 32, 33]:

$$\mathrm{DPCI} = \frac{1}{n}\left[n + 1 - 2\frac{\sum_{i=1}^{n}(n+1-i)y_i}{\sum_{i=1}^{n} y_i}\right], \tag{1}$$

where n is the number of rainy days in a year, y_i is precipitation in ith rainy day (mm), and $y_i \le y_{i+1}$. The day with precipitation over 0.1 mm defined as a rainy day in meteorology was used to separate rainy and rainless days [34].

3.2. Trend Test. The Mann–Kendall (MK) test is a nonparametric test method proposed by Mann and Kendall [35], which widely was used to evaluate statistically significant trends in hydro-meteorological time series. For a time series

Table 1: Description of 51 meteorological stations of the Hai River basin.

Station names (Abbr.)	Station numbers	Latitude (°N)	Longitude (°E)	Elevation (m)	Data series
Zhangbei (ZB)	53399	41.15	114.70	1393.3	1956–2018
Youyu (YY)	53478	40.00	112.45	1345.8	1957–2018
Datong (DT)	53487	40.08	113.42	1052.6	1955–2018
Tianzhen (TZ)	53490	40.43	114.05	1014.7	1957–2018
Shuozhou (SZ)	53578	39.37	112.43	1114.8	1957–2018
Daixian (DX)	53579	39.02	112.90	859.7	1957–2018
Wutaishan (WTS)	53588	38.95	113.52	2209.3	1956–2018
Yuxian (YX)	53593	39.83	114.57	910.5	1954–2018
Lingqiu (LQ)	53594	39.45	114.18	938.7	1971–2018
Yuanping (YP)	53673	38.73	112.72	828.2	1954–2018
Pingding (PD)	53687	37.78	113.63	753.0	1972–2018
Shijiazhuang (SJZ)	53698	38.07	114.35	103.6	1955–2018
Taigu (TG)	53775	37.42	112.60	786.7	1959–2018
Yushe (YS)	53787	37.07	112.98	1042.3	1957–2018
Xingtai (XT)	53798	37.07	114.50	78.5	1954–2018
Anze (AZ)	53877	36.17	112.25	861.0	1957–2018
Changzhi (CZ)	53882	36.07	113.03	1046.9	1973–2018
Xiangyuan (XY)	53884	36.52	113.03	877.9	1957–2018
Anyang (AY)	53898	36.05	114.13	194.8	1951–2018
Xinxiang (XX)	53986	35.32	113.88	73.2	1951–2018
Linxi xian (LXX)	54115	43.63	118.03	825.0	1952–2018
Duolunxian (DLX)	54208	42.18	116.47	1245.4	1952–2018
Fengning (FN)	54308	41.20	116.63	736.3	1956–2018
Weichang (WC)	54311	41.97	117.77	893.8	1951–2018
Zhangjiakou (ZJK)	54401	40.77	114.92	772.8	1956–2018
Huailai (HL)	54405	40.42	115.50	570.9	1954–2018
Yanqing (YQ)	54406	40.45	115.97	487.9	1959–2018
Miyun (MY)	54416	40.38	116.87	71.8	1957–2018
Chengde (CD)	54423	40.97	117.92	422.3	1951–2018
Zunhua (ZH)	54429	40.20	117.95	54.9	1956–2018
Qinglong (QL)	54436	40.42	118.95	255.4	1957–2018
Qinhuangdao (QHD)	54449	39.85	119.52	2.4	1954–2018
Jianchang (JC)	54452	40.80	119.82	365.5	1959–2018
Beijing (BJ)	54511	39.80	116.47	31.3	1951–2018
Bazhou (BZ)	54518	39.17	116.40	8.9	1957–2018
Baodi (BD)	54525	39.73	117.28	5.1	1959–2018
Tianjin (TJ)	54527	39.08	117.05	3.5	1951–2018
Tangshan (TS)	54534	39.65	118.10	23.2	1957–2018
Caofeidian (CFD)	54535	39.28	118.47	3.2	1956–2018
Laoting (LT)	54539	39.43	118.88	8.5	1957–2018
Baoding (BDG)	54602	38.73	115.48	16.8	1955–2018
Raoyang (RY)	54606	38.23	115.73	19.0	1957–2018
Botou (BT)	54618	38.08	116.55	13.2	1957–2018
Tanggu (TGG)	54623	39.05	117.72	4.8	1951–2018
Huanghua (HH)	54624	38.40	117.32	4.5	1956–2018
Nangong (NG)	54705	37.37	115.38	28.6	1958–2018
Lingxian (LX)	54715	37.32	116.57	18.6	1962–2018
Huimin (HM)	54725	37.50	117.53	11.7	1951–2018
Kenli (KL)	54744	37.58	118.55	8.5	1967–2018
Shenxian (SX)	54808	36.23	115.63	39.1	1957–2018
Jinan (JN)	54823	36.60	117.00	171.2	1951–2018

$X = \{x_1, x_2, \ldots, x_i, \ldots, x_m\}$ ($m > 10$), the MK test statistic Z is calculated as follows [36]:

$$Z = \begin{cases} \dfrac{S-1}{\sqrt{\mathrm{Var}(S)}}, & S > 0, \\ 0, & S = 0, \\ \dfrac{S+1}{\sqrt{\mathrm{Var}(S)}}, & S < 0. \end{cases} \quad (2)$$

In which,

$$S = \sum_{i=2}^{m} \sum_{j=1}^{i-1} \mathrm{Sgn}\left(x_i - x_j\right), \quad (3)$$

where $\mathrm{Sgn}(\theta)$ is equal to 1, 0, or −1 when θ is greater than, equal to, or less than 0, respectively; $\mathrm{Var}(S)$ is variance of S and can be calculated by the following formula:

$$\mathrm{Var}(S) = \frac{m(m-1)(2m+5)}{18}. \quad (4)$$

For the MK test, the positive value of Z represents an upward trend and the negative value represents a downward trend. If $|Z|$ is greater than 1.64, 1.96, and 2.57, the trends of X have significance levels of 10%, 5%, and 1%, respectively. More detailed procedures of the MK test can be found in the study by Shi et al. [10].

3.3. Abrupt Change Analysis. The Pettitt (P) test developed by Pettitt (1979) was used to determine the occurrence of a change point in this paper. For a time series $X = \{x_1, x_2, \ldots, x_i, \ldots, x_m\}$, the P test statistic U is calculated as follows [16, 37, 38]:

$$U_t = U_{t-1} + \sum_{i=1}^{m} \mathrm{Sgm}\left(x_t - x_i\right), \quad (5)$$

where $\mathrm{Sgm}(\phi)$ is equal to 1, 0, or −1 when ϕ is greater than, equal to, or less than 0, respectively; $t = 2, 3, \ldots, m$. Its statistic Z_t and the associated probabilities used in the significance testing are calculated by the following equation as follows:

$$Z_t = \max_{1 \le t \le m} \left|U_t\right|, \qquad P = 2\exp\left(\frac{-6Z_t^2}{m^2 + m^3}\right). \quad (6)$$

If P is less than 0.05, a significant change point exists [37].

4. Results

4.1. Spatial Distribution of Average DPCI Values. The annual DPCI values were calculated for 51 meteorological stations in the HRB for the period from 1951 to 2018. The average PDCI across almost every decade years and all the years, for each of 51 stations separately, is listed in Table 2. The average PDCI for 51 stations during 1951–2018 ranges between 0.6471 and 0.7938. The highest value of the DPCI is recorded at Beijing (BJ) station, which suffered the heaviest rainstorm of recent 61 years in July, 2012. On the contrary, the lowest value of the DPCI occurs at Datong (DT) station in the northwest of the basin. Through the analysis of the DPCI value in different periods, the following were found: (1) the average DPCI value of Beijing (BJ) station is at a higher value, and the lowest value in different periods is greater than 0.768, but that of Datong (DT) station is at a low value, and the highest value is less than 0.671; (2) the average DPCI value of Beijing (BJ) station as the highest value appeared in the 1950s, 1960s, and 2010s, and that of Datong (DT) station as the lowest value appeared in the 1950s, 1990s, 2000s, and 2010s; and (3) the highest average DPCI value (0.8242) appeared in Beijing (BJ) station in 1960s, but the lowest one (0.6156) appeared in Datong (DT) station in 2010s.

The DPCI values during 1951–2018 for each grid cell (30 m × 30 m) over HBR were spatially interpolated by the IDW method from 51 stations (Figure 2(h)). For the most part, high DPCI values, with averages of 0.70 in different periods, are found in eastern regions where high precipitation levels are recorded [23]. The spatial distribution characteristic of average DPCI is consistent in different periods. The DPCI values in the central and southern parts over the HRB exceed 0.675, which is consistent with the result of the study by Tong et al. [39]. There are four discrete high-value regions of DPCI, which are controlled by the Beijing (BJ) and Tianjin (TJ) stations in the Bohai Bay, Weichang (WC), and Chengde (CD) station in the northeast, Huimin (HM) station in the south, and Xinxiang (XX) and Anyang (AY) stations in the southwest. The spatial values of DPCI showed a decreasing trend in different period (Figures 2(a)–2(g)). Before 1990, the downward trend of the DPCI was relatively small, but after that, the downward trend increased significantly.

Figure 3 shows the relationship between the geographical factors (latitude, longitude, and elevation) and multiyear DPCI at 51 stations over the HRB. The DPCI changes tend to be negatively related to the altitude with R^2 of 0.0065 (Figure 3(a)) and the elevation with R^2 of 0.2312(Figure 3(c)) but tend to be positively related to the longitude with R^2 of 0.1985 (Figure 3(b)) during 1951–2018. The lower the linear coefficients of determination (R^2) indicate the existence of a nonsignificant correlation between DPCI and altitude, longitude, and elevation. In general, the average DPCI values in different periods (Figure 2) decrease northward to high altitude (Figure 3(a)), decrease westward to low longitude (Figure 3(b)), which is consistent with the results in Central-Southern Chile [4], and decrease westward and northward to high elevation (Figure 3(c)), which is consistent with the results in the Yangtze River Delta, China [22].

4.2. Spatial Characteristics of Annual DPCI Trend. The annual DPCI values exhibit a varying temporal trend, which can be characterized as spatially heterogeneous among stations (Figure 4(a)). Exception without trend in Jianchang (JC) station, other stations show negative annual DPCI

Table 2: Values for the average DPCI for almost every decade years and whole period during 1951–2018 at 51 stations of HRB.

Names	1950s	1960s	1970s	1980s	1990s	2000s	2010s	1951–2018
ZB	0.6833	0.6931	0.6994	0.6697	0.6725	0.6704	0.6479	0.6769
YY	0.6865	0.6747	0.6685	0.6499	0.6639	0.6605	0.6402	0.6635
DT	0.6701	0.6552	0.6671	0.6464	0.6354	0.6394	0.6156	0.6471
TZ	0.6747	0.6666	0.6614	0.6462	0.6522	0.6462	0.6246	0.6532
SZ	0.6917	0.6775	0.6748	0.6626	0.6528	0.6719	0.6573	0.6697
DX	0.7109	0.6785	0.6821	0.6706	0.6744	0.6696	0.6597	0.6778
WTS	0.7039	0.6799	0.6890	0.6701	0.6675	0.6723	0.6769	0.6796
YX	0.6769	0.6730	0.6688	0.6617	0.6483	0.6440	0.6295	0.6576
LQ	0.6769	0.6581	0.6734	0.6459	0.6477	0.6549	0.6419	0.6569
YP	0.6912	0.6827	0.7008	0.6824	0.6731	0.6852	0.6848	0.6857
PD	0.7115	0.7022	0.6882	0.7031	0.6896	0.6857	0.6683	0.6927
SJZ	0.6852	0.6902	0.6791	0.6920	0.6826	0.6780	0.6590	0.6811
TG	0.7049	0.6921	0.6850	0.7041	0.6679	0.6775	0.6643	0.6851
YS	0.7158	0.6507	0.6636	0.6772	0.6582	0.6844	0.6516	0.6713
XT	0.7115	0.6985	0.6841	0.6878	0.6821	0.6782	0.6645	0.6866
AZ	0.7113	0.6686	0.6857	0.6784	0.6632	0.6705	0.6413	0.6741
CZ	0.7192	0.6759	0.6751	0.6823	0.6765	0.6836	0.6567	0.6811
XY	0.7076	0.6657	0.6666	0.6830	0.6498	0.6575	0.6445	0.6676
AY	0.8096	0.8082	0.7959	0.7980	0.7925	0.7759	0.7482	0.7901
XX	0.7925	0.7956	0.7920	0.8062	0.7989	0.7777	0.7428	0.7871
LXX	0.7652	0.7875	0.7843	0.7848	0.7740	0.7719	0.7356	0.7725
DLX	0.6777	0.6734	0.6700	0.6614	0.6650	0.6404	0.6648	0.6645
FN	0.6892	0.7020	0.6920	0.6801	0.6791	0.6654	0.6790	0.6838
WC	0.7731	0.7776	0.7749	0.7608	0.7615	0.7074	0.7180	0.7536
ZJK	0.6859	0.6721	0.6760	0.6578	0.6484	0.6453	0.6375	0.6604
HL	0.7079	0.7175	0.6925	0.6742	0.6803	0.6749	0.6654	0.6876
YQ	0.7047	0.6983	0.7006	0.6686	0.6667	0.6491	0.6365	0.6751
MY	0.7193	0.7040	0.7135	0.6921	0.6841	0.6623	0.6862	0.6943
CD	0.7809	0.7644	0.7696	0.7697	0.7480	0.7414	0.7208	0.7565
ZH	0.7015	0.6989	0.6999	0.6939	0.6856	0.6780	0.7009	0.6939
QL	0.7111	0.7184	0.7124	0.6892	0.7000	0.6822	0.7053	0.7025
QHD	0.6910	0.7046	0.7113	0.7025	0.7056	0.6815	0.6977	0.6993
JC	0.7070	0.7073	0.7154	0.7006	0.7120	0.6965	0.7129	0.7073
BJ	0.8194	0.8242	0.8114	0.7871	0.7774	0.7683	0.7689	0.7938
BZ	0.7127	0.7268	0.7254	0.7048	0.6808	0.6958	0.6873	0.7049
BD	0.7064	0.7338	0.7166	0.7040	0.6760	0.6846	0.6878	0.7014
TJ	0.7928	0.8123	0.8089	0.7921	0.7592	0.7804	0.7391	0.7841
TS	0.7079	0.7169	0.7187	0.7001	0.6908	0.6783	0.6885	0.7002
CFD	0.7143	0.7318	0.7313	0.7243	0.7075	0.6861	0.6919	0.7127
LT	0.7177	0.7330	0.7458	0.7242	0.7159	0.7036	0.6994	0.7203
BDG	0.7127	0.7314	0.7213	0.7461	0.6953	0.6759	0.6666	0.7075
RY	0.7098	0.7156	0.6968	0.7161	0.6798	0.6734	0.6697	0.6946
BT	0.7061	0.7171	0.7039	0.7216	0.6720	0.6666	0.6744	0.6946
TGG	0.7740	0.8117	0.8129	0.8039	0.7892	0.7715	0.7560	0.7891
HH	0.7054	0.7186	0.7278	0.7243	0.6830	0.7014	0.6888	0.7073
NG	0.7010	0.7007	0.6920	0.7101	0.6797	0.6757	0.6677	0.6897
LX	0.6936	0.6868	0.6906	0.7155	0.6917	0.6778	0.6792	0.6909
HM	0.7850	0.8091	0.8008	0.7911	0.7828	0.7554	0.7282	0.7795
KL	0.7132	0.7143	0.7146	0.7186	0.7056	0.6846	0.6853	0.7053
SX	0.6873	0.6969	0.6834	0.6967	0.6847	0.6825	0.6539	0.6840
JN	0.7605	0.7852	0.7768	0.7843	0.7825	0.7639	0.7134	0.7675

trends, of which 5 stations have the trend greater than 0.001/a, 15 stations have the trend between 0.0007/a and 0.00099/a, 25 stations have the trend between 0.0004/a and 0.00069/a, and the trends of the remaining stations are less than 0.00039/a. Based on the MK test, the annual DPCI trends are also tested, and the results are shown in Figure 4(b). For the annual DPCI trend, more than 80% of the stations show significant changes at a 0.1 significance level. Among them, 37 out of 41 stations exhibit significant trends at a 0.05 significance level ($|Z| > 1.96$), and 29 out of 41 stations are dominated by a significant trend at a 0.01 significance level ($|Z| > 2.57$). The analysis results are consistent with those of Tong et al. that the daily precipitation concentrations at most stations in North China show a significant downward trend from 1960 to 2011 [39].

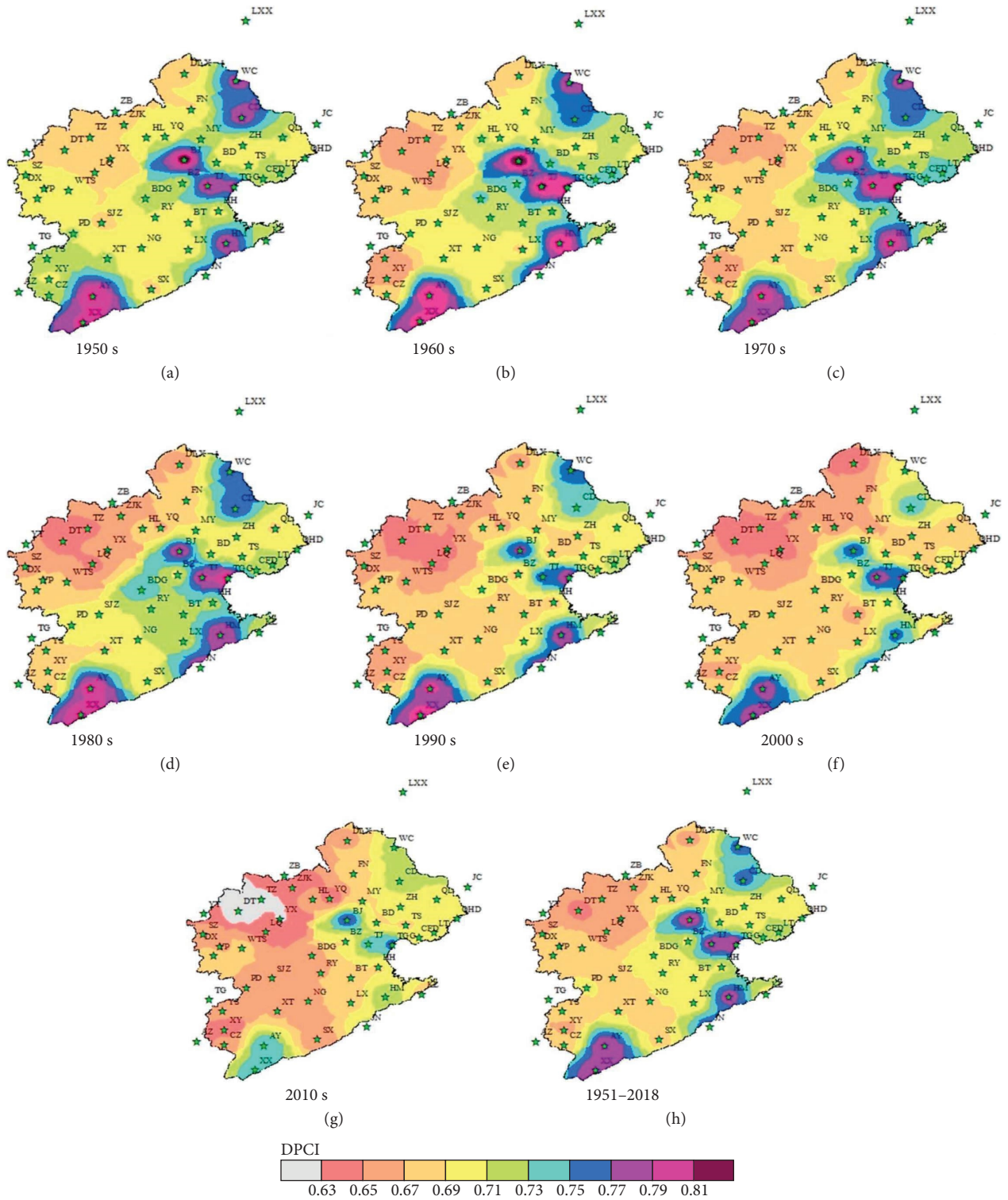

Figure 2: Spatial distributions of the mean DPCI in different periods.

4.3. Spatial Characteristics of Abrupt Change of Annual DPCI. Figure 5 shows the possible abrupt change of annual DPCI based on the Pettitt test from 1951 to 2018. In all records, there are 22 out of 51 stations with statistically significant change points at the significant level of 5%. Meanwhile, abrupt changes are more likely to occur during the 1980s, accounting for 47.06% of all stations, followed by those occurring during the 1970s (17.65%).

There is a postponement trend, in which abrupt changes move from west to east with time. Before 1970, there were only three stations with a change point, namely, Changzhi (CZ) Station at 1958, Yushe (YS) Station at 1959, and Xingtai

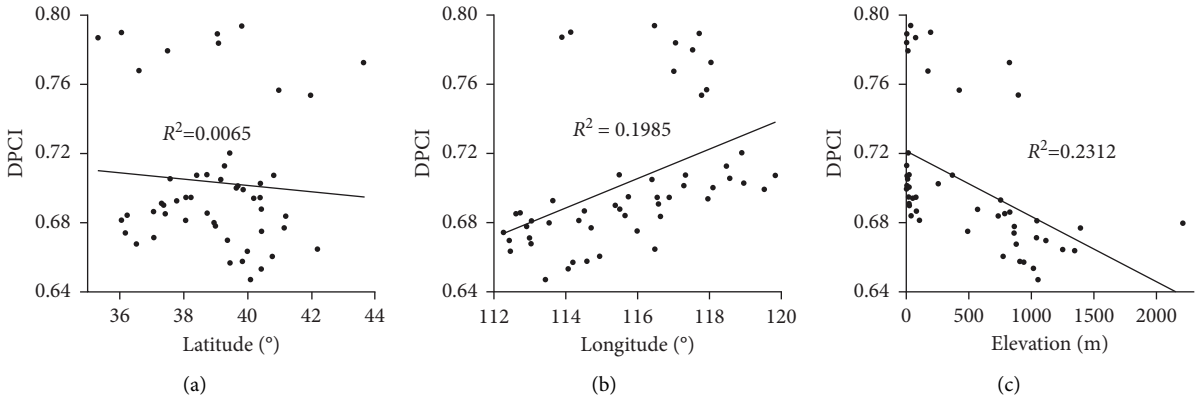

Figure 3: The multiyear average PDCI versus latitude (a), longitude (b), and elevation (c) at 51 stations over the HRB.

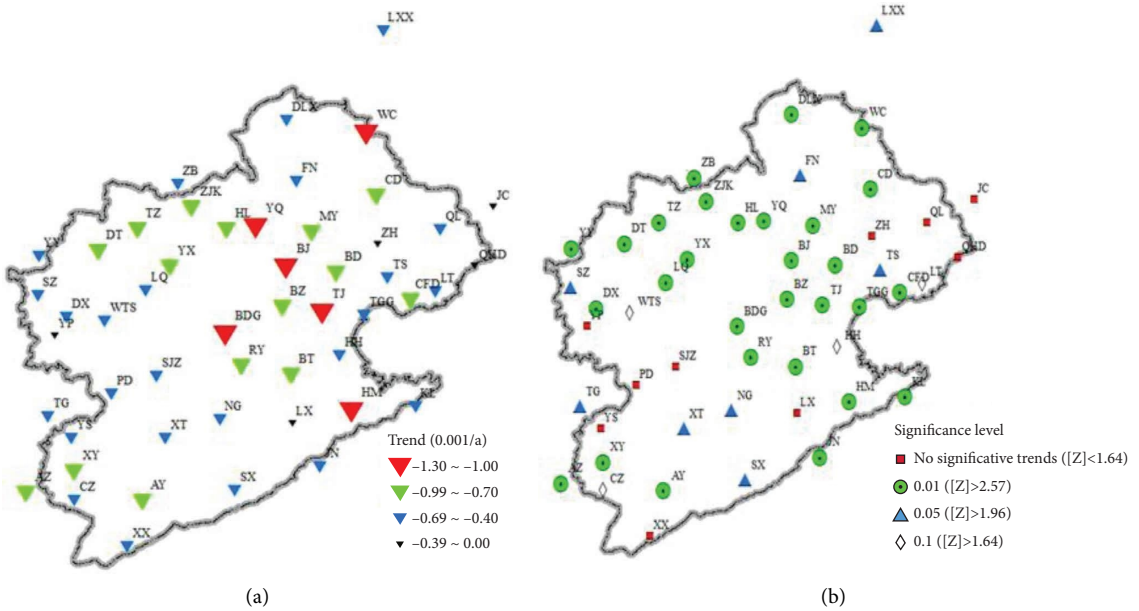

Figure 4: Spatial trend variations of annual DPCI (a) and MK test (b) at 51 stations.

(XT) Station at 1964, which were located in the southwest of the HRB and fail to pass the significant level of 5%. After 1990, there are 15 stations with a change point, which are mostly distributed at the southern and eastern edges of the HRB.

5. Discussion

5.1. Comparison between the Results in the HRB and Other Areas of China. To understand the characteristic of the DPCI in the HBR, we collected published study results from other regions of China (Table 3). The DPCI of the HRB range from 0.64 to 0.79 is relatively close to the Huai River basin (0.64–0.72) but greatly lower than the Pearl River basin (0.74–0.80). Table 3 indicates that DPCIs of the Lancang River basin, Xinjiang and Shanxi provinces are 0.57–0.73, 0.58–0.70, and 0.59–0.64, respectively, which are lower than those of northeast China (0.64–0.70), The Huai River basin (0.64–0.72) and the Hai River basin (0.64–0.79). However, the DPCI of the Pearl River basin with range between 0.74 and 0.80 is largest in Table 3. These findings confirm the characteristic that the eastern DPCIs are higher than the eastern DPCIs in China and the DPCIs in south China and north China are relatively large.

5.2. The Influence of Data Length on the Characteristics of DPCI. It can be seen from the abovementioned that the temporal and spatial distribution characteristics of DPCI in the HRB are based on the daily precipitation data of 51 stations from 1951 to 2018. However, how do the characteristics of the DPCI depend on the length of the time series? To describe the impact of the data length on the characteristics of the DPCI, the following two indicators are defined.

$$\begin{aligned}\text{Max } EP_n &= \max_{1\le m\le M}\left|\text{Mean\_DPCI}_{m,n} - \text{Mean\_DPCI}_{m,n-1}\right|,\\ \text{Max } ET_n &= \max_{1\le m\le M}\left|\text{Trend\_DPCI}_{m,n} - \text{Trend\_DPCI}_{m,n-1}\right|,\end{aligned} \tag{7}$$

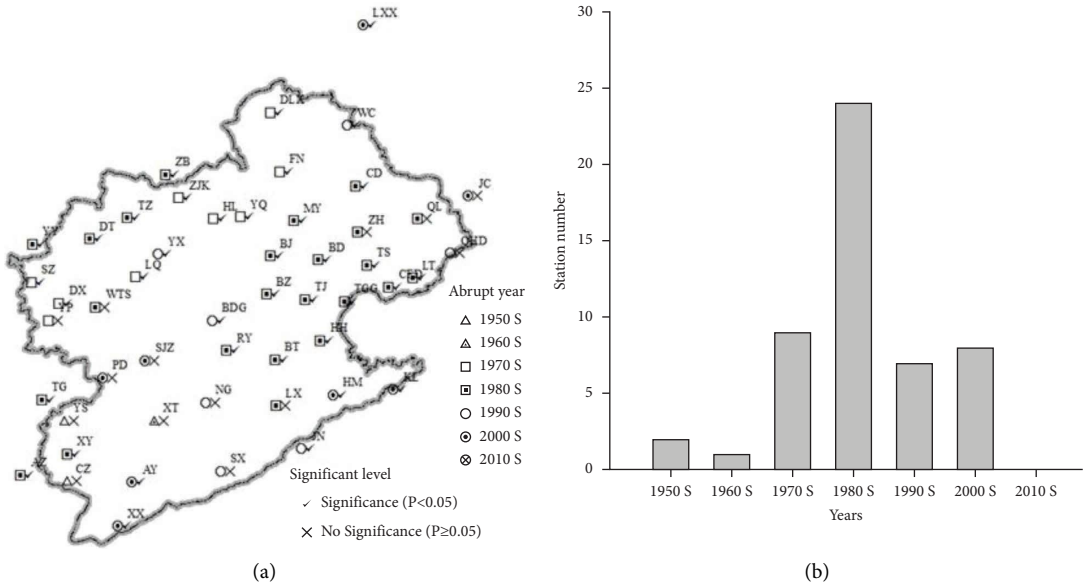

Figure 5: Spatial abrupt years (a) and statistical results (b) of annual DPCI at 51 stations.

Table 3: Comparison of DPCI between different regions in China.

Sources	Study regions	Number of stations	Periods	Range of DPCI
Zhang et al. [17]	Pearl River basin	42	1960–2005	0.74–0.80
Li et al. [18]	Xinjiang province	50	1961–2008	0.58–0.70
Shi et al. [10]	Lancang River basin	31	1960–2010	0.57–0.73
Shi et al. [19]	Huai River basin	38	1951–2010	0.64–0.72
Yuan et al. [20]	Shanxi province	14	1957–2014	0.59–0.64
Wang et al. [21]	Northeast China	71	1961–2016	0.64–0.70
This study	Hai River basin	51	1951–2018	0.64–0.79

where MaxEP_n is the maximum change value of the annual average DPCI from $n-1$ to n years for all stations in the HRB; MaxET_n is the maximum change value of the DPCI trend from $n-1$ to n years for all stations in the HRB; Mean_$DPCI_{m,n}$ is the average DPCI of mth station from 1 to nth year; M is the number of station in the HRB and is equal to 58 in the paper; Trend_$DPCI_{m,n}$ is the DPCI trend of mth station from 1 to nth year. The serial number of year 1, 2, ..., 68 is corresponding to 1951, 1952, ..., 2018, respectively.

Figure 6 shows that the MaxEP and MaxET decrease with the increase of the data length and converge to a smaller interval. After 2000, the range of MaxEP is from 0.00086 to 0.00265 with the mean value of 0.0016, which accounts for 0.23% of multiyear average PDCI (0.7032) from 1951 to 2018 in the HRB. Similarly, the range of MaxEP is from 0.00086 to 0.00265 with the mean value of 0.00015, which accounts for 2.34% of average Trend (−0.00641) from 1951 to 2018 in the HRB. That is to say, the spatial and temporal variability of the DPCI based on the time series over 50 years can represent the distribution characteristics of the DPCI in the HRB. However, compared with the spatial distribution (corresponding to the multiyear average DPCI), the temporal distribution (corresponding to the trend of DPCI) more greatly depends on the length of the time series.

5.3. Relationship between Short and Long Term Precipitation Patterns. Figure 7 shows that the higher that the DPCI will be, the higher proportion of the annual total precipitation (PTP) that falls on the rainiest days at a station. 5% of the rainiest days accounts for 30.26–45.79% of the total rainfall, 10% for 46.54–65.24%, 15% for 58.47–76.70%, 20% for 67.35–84.04%, 25% for 74.17–89.23%, and 30% for 79.70–92.76%. The linear coefficients of determination (R^2) between the DPCIs and the PTPs for 5%, 10%, 15%, 20%, 25%, and 30% were 0.9747, 0.9906, 0.9963, 0.9988, 0.9989, and 0.9980, respectively. The daily precipitation heterogeneity over a year is dominated by percentages of precipitation amount provided by the highest quartile of rainy days or large daily amount of precipitation [19]. Due to 25% of the rainiest days with the highest R^2 of 0.9989, the daily heterogeneity of the rainfall within a year can be best accounted by the PTP contributed by 25% of the rainiest days in the HRB.

Figure 8 shows that the DPCI changes tend to be positively related to annual precipitation amount with R^2 of 0.1612 but negatively relate to the annual precipitation day with R^2 of 0.0146 during 1951–2018. In other words, more annual precipitation amount means higher daily heterogeneity, and less annual precipitation day means higher daily heterogeneity. Thus, a few very rainy days can change a year's rainfall total and dry or wet situation. The

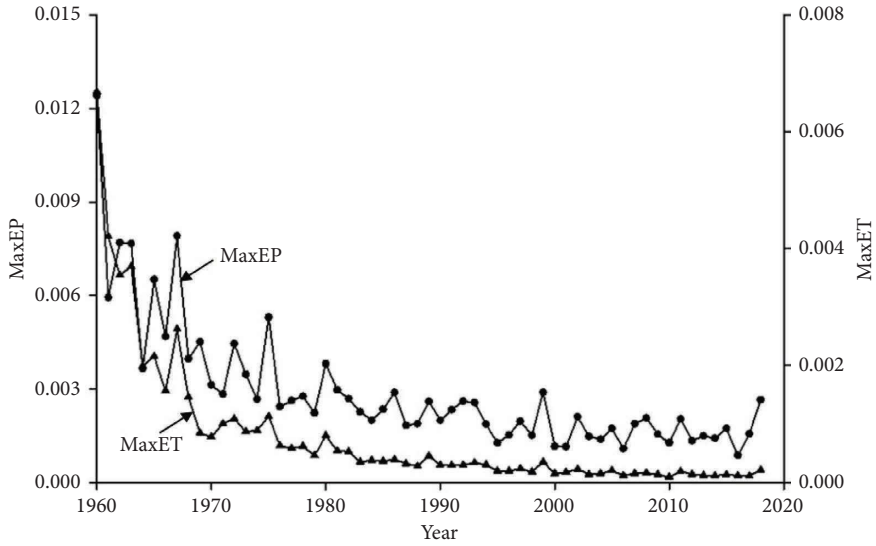

Figure 6: The Max*EP* and Max*ET* change with year.

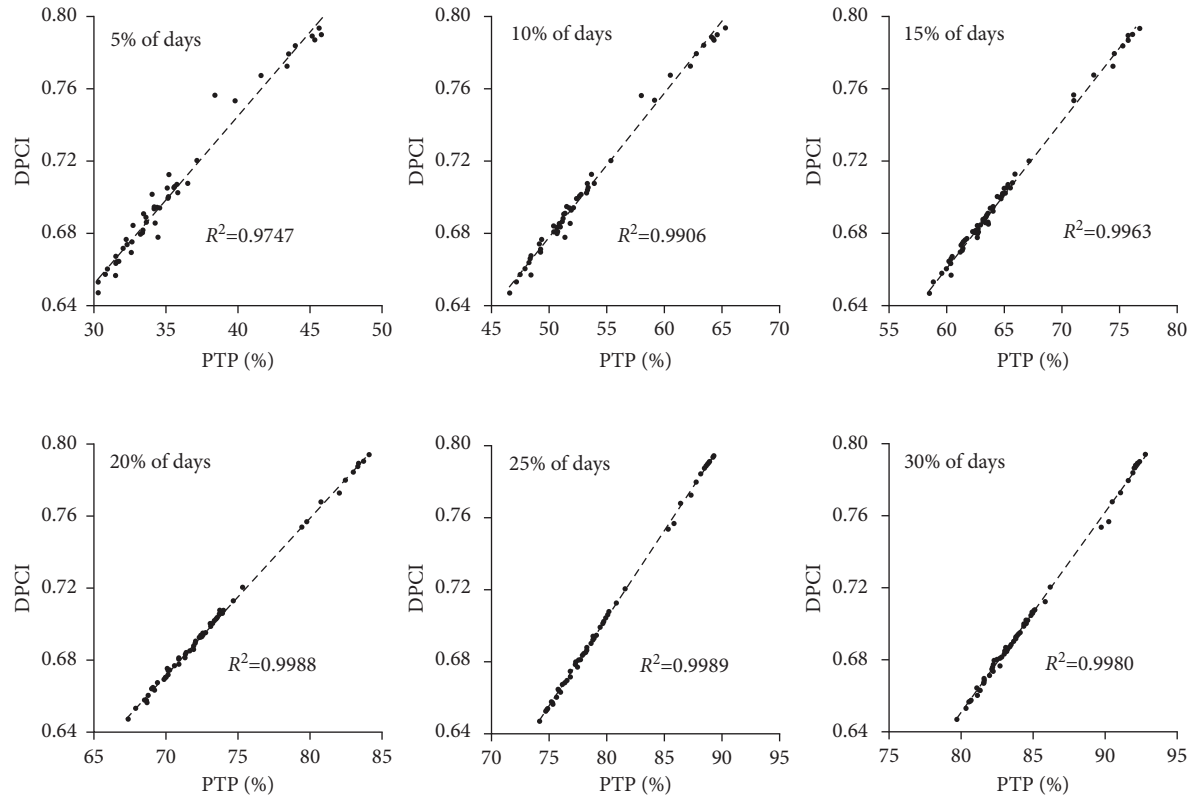

Figure 7: The multiyear average PDCI versus the PTP contributed by 5–30% of the rainiest days for 51 stations over the HRB.

lower precipitation levels based on higher daily heterogeneity indicate a higher risk of drought in I region, and the higher precipitation levels coupled with relatively higher PDCIs would increase the risk of flood in II region [21]. For example, at Weichang (WC) station with the higher daily rainfall heterogeneity (multiyear DPCI of 0.7536) and the lower annual precipitation amount (455.28 mm) in I region, precipitation amount within 25% of the rainiest days (about 32 days) is 388.63 mm; then, the precipitation amount in the remaining 333 days of the year is only 66.65 mm, which is bound to cause a higher drought risk. However, at Beijing (BJ) station with the highest daily rainfall heterogeneity (multiyear DPCI of 0.7938) and the higher annual precipitation amount (591.12 mm) in II region, precipitation amount within 5% of the rainiest days (about 5 days) is 269.79 mm, and the daily precipitation amount reaches 53.99 mm, which can easily lead to flood disaster. As a whole, a high

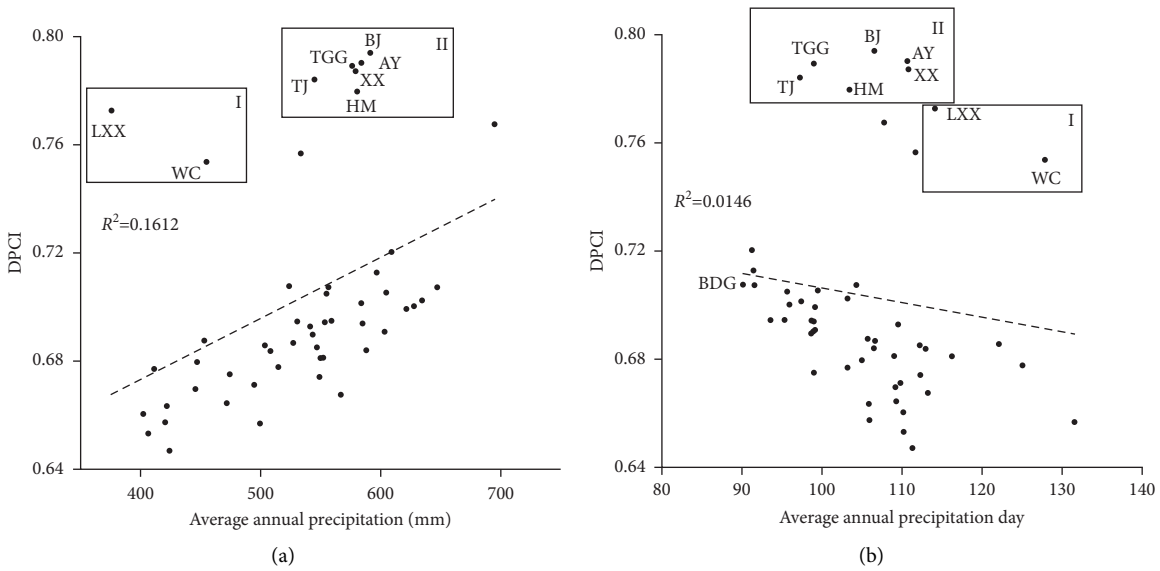

Figure 8: The multiyear average PDCI versus annual total precipitation (a) and annual total precipitation day (b) at 51 stations over the HRB.

value of the DPCI mainly indicates that drought and flood disasters are more frequent in I region and II region, respectively.

5.4. Relationship between Disaster Losses and DPCI. To further explore the possible natural disasters associated with high DPCI value, the relationships between flood and drought losses and annual DPCI are analyzed based on the linear correlation analysis. The higher DPCI values lead to greater flood losses with the R^2 of 0.3883 (Figure 9(a)) and more drought losses with the R^2 of 0.1358 (Figure 9(b)). The DPCI value in flood years is much greater than that in drought years, and the loss of flood disasters is also much greater than that of drought disasters. Flood or drought disasters with higher DPCI value are closely related to the annual precipitation. Generally speaking, in a dry year, when the precipitation anomaly is negative, it is easy to cause drought losses, while in wet years, when the precipitation anomaly is positive, it tends to cause flood losses (Figure 9(c)). For flood losses, although the annual precipitation was only 588.32 mm in 1963, the highest DPCI value led to the greatest flood loss. However, the annual precipitation reached 812.97 mm in 1964, which was the highest annual precipitation during 1951–2018, while the relatively lower DPCI value led to the smaller flood loss. For drought losses, the higher DPCI value coupled with the lower annual precipitation (442.78 mm) led to the greatest drought loss in 1981. Then, the lower DPCI value coupled with the lowest annual precipitation (350.29 mm) during 1951–2018 led to the greater drought loss in 1965. There are similar DPCI values in 1965 (0.6984) and in 1987 (0.7013), and the annual precipitation (561.49 mm) in 1987 is much higher than that (350.29 mm) in 1965. Then, the drought loss (22.92 billion yuan) in 1987 was greater than that (13.36 billion yuan) in 1965. The possible reason is that there were several consecutive wet years in the early 1965, resulting in higher soil moisture content. In addition, the regulation and storage of water conservancy projects reduced the drought losses.

5.5. Trend Analysis of Flood and Drought Disasters. To understand the risk of flood and drought in the HRB in the future, the relationships between the average annual DPCI and annual DPCI trend (Figure 10(a)) and between the average annual precipitation and annual precipitation trend (Figure 10(b)) are analyzed based on 51 stations over the HRB. We would analyze the risk of flood and drought disasters of the HRB from two perspectives. First, the stations show the negative trends of annual DPCI except for Jianchang (JC) station during 1951–2018, and a greater downward trend is accompanied by the higher average annual DPCI values with the R^2 of 0.0763 (Figure 9(a)). The annual DPCI value of each station would decrease, and the differences of annual DPCI among different stations may become smaller and smaller. The risk of local flood disasters would be gradually reduced in the future [24]. Second, the stations show the negative trends of annual precipitation except for Jinan (JN) and Weichang (WC) stations during 1951–2018. The higher change rate appears in stations where the average annual precipitation amounts are between 500 mm and 600 mm. Especially in Beijing station, the inter-annual variation rate of precipitation, reaching −3.16 mm/a, is the largest and passes the 0.1 significance level based on the MK method. The risk of regional drought disasters would become more serious [40, 41]. In the future, the risk of flood disasters would be reduced, but the drought disasters would be increased in the HRB. Especially in the mega cities, with the social and economic development, the demand for water resources will increase, which will further exacerbate the contradiction between supply and demand of water resources.

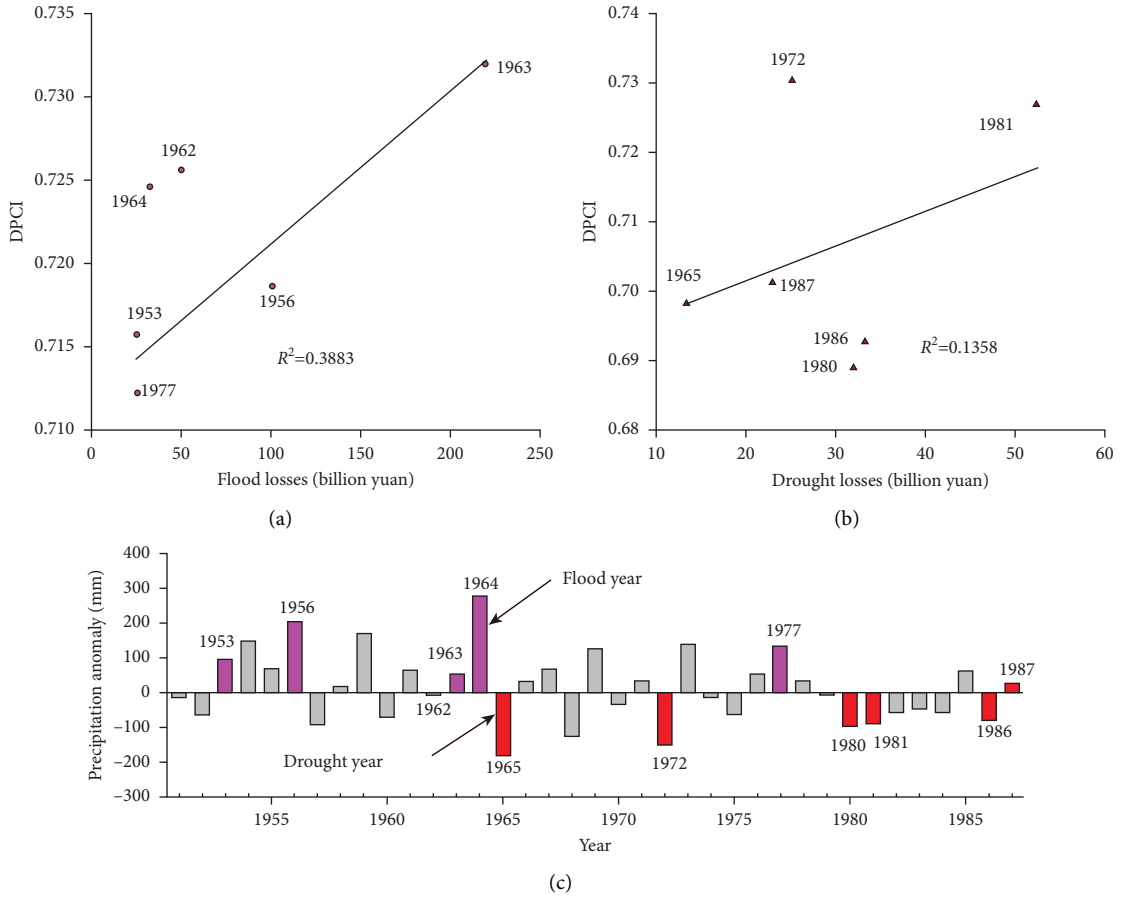

Figure 9: The PDCI versus flood (a) and drought (b) losses before 1990 and corresponding annual precipitation anomaly (c) over the HRB.

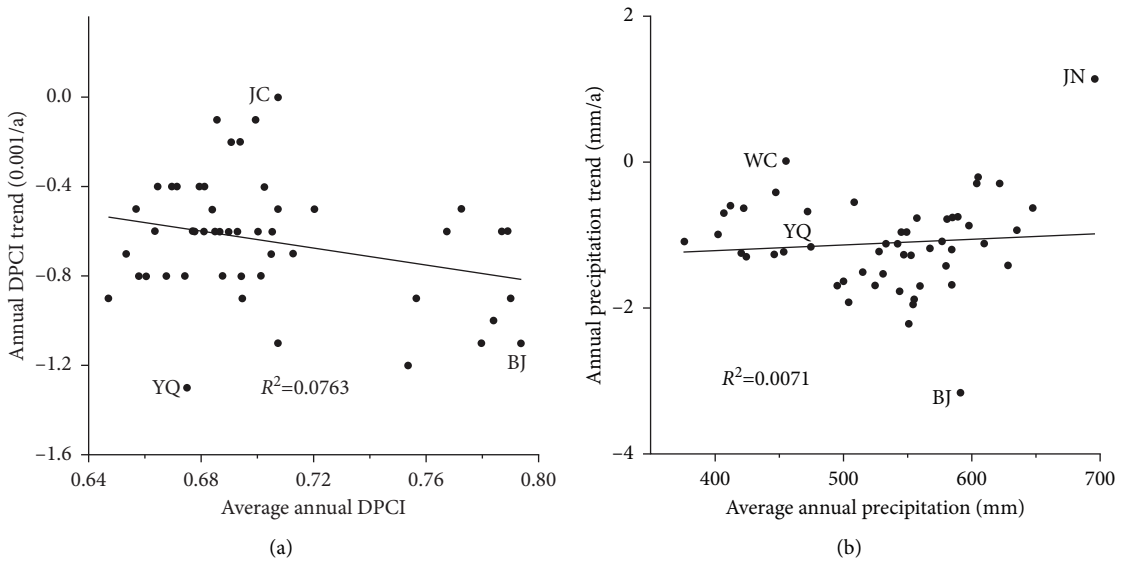

Figure 10: The average PDCI versus DPCI trend (a) and the average precipitation versus precipitation trend (b) at 51 stations over the HRB.

6. Conclusion

In this study, we set up the DPCI based on the Gini coefficient and analyzed spatial and temporal variability of the DPCI based on the Mann–Kendall and Pettitt tests in the HRB. The results of the time series of the DPCI from 1951 to 2018 show that the high values of the multiyear average DPCI are mainly situated in the southern and eastern parts, that the stations show DPCI trends except for Jianchang (JC) station, and that the abrupt changes are

concentrated in 1980s accounting for 47.06% for 51 stations.

The higher DPCI is greatly correlated with the higher PTP that falls on the rainiest days at a station, and the higher DPCI values lead to greater flood or drought losses. The higher DPCI coupled with more precipitation is easy to cause flood disaster; conversely, the higher DPCI along with less precipitation is easy to cause drought disaster. In the future, the risk of flood disasters would be reduced, but the drought disasters would be increased in the HRB.

However, the correlation between the DPCI and disaster loss is still slight, which indicates that disaster loss may relate to soil moisture content, changes of underlying surface and disaster resilience, and so on. Understanding the relationships among them requires a more scientific knowledge of the geomorphological, hydrological, socioeconomic changes as a concrete basis for assessment of flood and drought risk and utilization of water resources.

Data Availability

(1) The daily precipitation data of 51 meteorological stations are provided by the National Climatic Center (NCC) of the China Meteorological Administration (CMA). (2) The loss data of flood and drought disasters data come from the "flood and drought disasters in the Haihe River Basin" composed by Haihe River Water Conservancy Commission, MWR.

Conflicts of Interest

The authors declare that they have no conflicts of interest.

Acknowledgments

This work was supported by the Open Research Fund of State Key Laboratory of Simulation and Regulation of Water Cycle in River Basin (China Institute of Water Resources and Hydropower Research), grant no. IWHR-SKL-KF201812.

References

[1] L. L. Shen, L. Lu, T. J. Hu, R. Lin, J. Wang, and C. Xu, "Homogeneity test and correction of daily temperature and precipitation data (1978–2015) in North China," *Advances in Meteorology*, vol. 2018, Article ID 4712538, 17 pages, 2018.

[2] F. V. Davenport and N. S. Diffenbaugh, "Using machine learning to analyze physical causes of climate change: a case study of U.S. Midwest extreme precipitation," *Geophysical Research Letters*, vol. 48, no. 15, 2021.

[3] G. Q. Tang, M. P. Clark, and S. M. Papalexiou, "The use of serially complete station data to improve the temporal continuity of gridded precipitation and temperature estimates," *Journal of Hydrometeorology*, vol. 22, no. 6, pp. 1553–1568, 2021.

[4] P. Sarricolea, Ó. Meseguer-Ruiz, R. Serrano-Notivoli, M. V. Soto, and J. Martin-Vide, "Trends of daily precipitation concentration in Central-Southern Chile," *Atmospheric Research*, vol. 215, pp. 85–98, 2019.

[5] K. E. Trenberth, "Changes in precipitation with climate change," *Climate Research*, vol. 47, no. 1, pp. 123–138, 2011.

[6] M. K. Van Aalst, "The impacts of climate change on the risk of natural disasters," *Disasters*, vol. 30, no. 1, pp. 5–18, 2006.

[7] X. J. Shen, B. H. Liu, and X. G. Lu, "Weak cooling of cold extremes versus continued warming of hot extremes in China during the recent global surface warming hiatus," *Journal of Geophysical Research: Atmospheres*, vol. 123, no. 8, pp. 4073–4087, 2018.

[8] T. Raziei, "An analysis of daily and monthly precipitation seasonality and regimes in Iran and the associated changes in 1951–2014," *Theoretical and Applied Climatology*, vol. 134, no. 3-4, pp. 913–934, 2018.

[9] T. Caloiero, R. Coscarelli, and R. Gaudio, "Spatial and temporal variability of daily precipitation concentration in the Sardinia region (Italy)," *International Journal of Climatology*, vol. 39, no. 13, pp. 5006–5021, 2019.

[10] W. L. Shi, X. Z. Yu, W. G. Liao, Y. Wang, and B. Jia, "Spatial and temporal variability of daily precipitation concentration in the Lancang River basin, China," *Journal of Hydrology*, vol. 495, pp. 197–207, 2013.

[11] N. Cortesi, J. C. Gonzalez-Hidalgo, M. Brunetti, and J. Martin-Vide, "Daily precipitation concentration across Europe 1971–2010," *Natural Hazards and Earth System Sciences*, vol. 12, no. 9, pp. 2799–2810, 2012.

[12] J. Suhaila and A. A. Jemain, "Spatial analysis of daily rainfall intensity and concentration index in Peninsular Malaysia," *Theoretical and Applied Climatology*, vol. 108, no. 1-2, pp. 235–245, 2012.

[13] S. Ghaedi and A. Shojaian, "Spatial and temporal variability of precipitation concentration in Iran," *Geographica Pannonica*, vol. 24, no. 4, pp. 244–251, 2020.

[14] E. Vyshkvarkova, E. Voskresenskaya, and J. Martin-Vide, "Spatial distribution of the daily precipitation concentration index in Southern Russia," *Atmospheric Research*, vol. 203, pp. 136–143, 2018.

[15] A. Vélez, J. Martin-Vide, D. Roye, and O. Santaella, "Spatial analysis of daily precipitation concentration in Puerto Rico," *Theoretical and Applied Climatology*, vol. 136, no. 3-4, pp. 1347–1355, 2019.

[16] P. Yang, Y. Y. Zhang, J. Xia, and S. Sun, "Investigation of precipitation concentration and trends and their potential drivers in the major river basins of Central Asia," *Atmospheric Research*, vol. 245, Article ID 105128, 2020.

[17] Q. Zhang, C. Y. Xu, M. Gemmer, Y. D. Chen, and C. Liu, "Changing properties of precipitation concentration in the Pearl River basin, China," *Stochastic Environmental Research and Risk Assessment*, vol. 23, no. 3, pp. 377–385, 2009.

[18] X. M. Li, F. Q. Jiang, L. H. Li, and G. Wang, "Spatial and temporal variability of precipitation concentration index, concentration degree and concentration period in Xinjiang, China," *International Journal of Climatology*, vol. 31, no. 11, pp. 1679–1693, 2011.

[19] P. Shi, X. Y. Qiao, X. Chen et al., "Spatial distribution and temporal trends in daily and monthly precipitation concentration indices in the upper reaches of the Huai River, China," *Stochastic Environmental Research and Risk Assessment*, vol. 28, no. 2, pp. 201–212, 2014.

[20] R. Q. Yuan, Y. N. Wang, P. Wang, and Y. Chen, "An analysis of precipitation concentration variation characteristics and influential factors in Shanxi province, China," *Climate Change Research*, vol. 14, no. 1, pp. 11–20, 2018.

[21] R. Wang, J. Q. Zhang, E. L. Guo, C. Zhao, and T. Cao, "Spatial and temporal variations of precipitation concentration and

their relationships with large-scale atmospheric circulations across Northeast China," *Atmospheric Research*, vol. 222, pp. 62–73, 2019.

[22] C. Mei, J. H. Liu, Z. Huang et al., "Spatiotemporal pattern variations of daily precipitation concentration and their relationship with possible causes in the Yangtze River Delta, China," *Journal of Water and Climate Change*, vol. 13, no. 3, pp. 1583–1598, 2022.

[23] L. N. Wang, H. H. Zhu, and F. Lu, "Characteristics of temporal and spatial variation of precipitation in Haihe River Basin during recent 50 years," *Agricultural Research in the Arid Areas*, vol. 30, no. 02, pp. 242–246, 2012, (In Chinese).

[24] X. F. Liu, L. Xiang, and C. W. Yu, "Characteristics of temporal and spatial variations of the precipitation extremes in the Haihe River Basin," *Climatic and Environmental Research*, vol. 15, no. 4, pp. 451–461, 2010, (In Chinese).

[25] M. Y. Ma, Y. P. Han, and Q. M. Wang, "Temporal and spatial variations of extreme precipitation in the Haihe River Basin and its relationship with atmospheric circulation indexes," *Water Resources and Power*, vol. 37, no. 6, pp. 1–4, 2019, (In Chinese).

[26] Z. Z. Jia, S. M. Liu, Z. W. Xu, Y. Chen, and M. Zhu, "Validation of remotely sensed evapotranspiration over the Hai River Basin, China," *Journal of Geophysical Research: Atmospheres*, vol. 117, no. 13, 2012.

[27] X. L. Liu, "By sector water consumption and related economy analysis integrated model and its application in Hai River Basin, China," *Journal of Water Resource and Protection*, vol. 4, no. 5, pp. 264–276, 2012.

[28] F. W. Chen and C. W. Liu, "Estimation of the spatial rainfall distribution using inverse distance weighting (IDW) in the middle of Taiwan," *Paddy and Water Environment*, vol. 10, no. 3, pp. 209–222, 2012.

[29] Haihe River Water Conservancy Commission MWR, *Flood and Drought Disasters in the Haihe River Basin*, Tianjin Science and Technology Press, Tianjin, China, 2009.

[30] R. Monjo and J. Martin-Vide, "Daily precipitation concentration around the world according to several indices," *International Journal of Climatology*, vol. 36, no. 11, pp. 3828–3838, 2016.

[31] M. O. Lorenz, "Methods of measuring the concentration of wealth," *Publications of the American Statistical Association*, vol. 9, no. 70, pp. 209–219, 1905.

[32] K. Rajah, T. O'Leary, A. Turner, G. Petrakis, M. Leonard, and S. Westra, "Changes to the temporal distribution of daily precipitation," *Geophysical Research Letters*, vol. 41, no. 24, pp. 8887–8894, 2014.

[33] Y. X. Yin, H. S. Chen, G. J. Wang, W. Xu, S. Wang, and W. Yu, "Characteristics of the precipitation concentration and their relationship with the precipitation structure: a case study in the Huai River basin, China," *Atmospheric Research*, vol. 253, Article ID 105484, 2021.

[34] P. Frich, L. V. Alexander, P. Della-Marta et al., "Observed coherent changes in climatic extremes during the second half of the twentieth century," *Climate Research*, vol. 19, no. 3, pp. 193–212, 2002.

[35] M. G. Kendall, *Rank Correlation Methods*, Charles Griffin, London, UK, 1975.

[36] A. A. Fenta, H. Yasuda, K. Shimizu, and N. Haregeweyn, "Response of streamflow to climate variability and changes in human activities in the semiarid highlands of northern Ethiopia," *Regional Environmental Change*, vol. 17, no. 4, pp. 1229–1240, 2017.

[37] Z. M. Ma, S. Z. Kang, L. Zhang, L. Tong, and X. Su, "Analysis of impacts of climate variability and human activity on streamflow for a river basin in arid region of northwest China," *Journal of Hydrology*, vol. 352, no. 3-4, pp. 239–249, 2008.

[38] X. P. Zhang, L. Zhang, J. Zhao, P. Rustomji, and P. Hairsine, "Responses of streamflow to changes in climate and land use/cover in the Loess Plateau, China," *Water Resources Research*, vol. 44, no. 7, Article ID W00A07, 2008.

[39] X. H. Tong, X. P. Liu, Q. Y. Jia, and B. Jia, "Spatial and temporal variability of daily precipitation concentration in China during 1960–2011," *Climatic and Environmental Research*, vol. 22, no. 3, pp. 301–314, 2017, (In Chinese).

[40] X. Zhang, Y. Hua, J. Feng et al., "The evolution characteristics of drought and the analysis of rainfall intensity probability during alternating dry–wet change in the haihe river basin," *Applied Ecology and Environmental Research*, vol. 16, no. 5, pp. 6395–6407, 2018.

[41] B. Tang, W. T. Hu, and A. M. Duan, "Assessment of extreme precipitation indices over Indochina and South China in CMIP6 models," *Journal of Climate*, vol. 34, no. 18, pp. 7507–7524, 2021.